Visual Feedback Gain Modulates the Activation of Task-Related Networks and the Suppression of Non-Task Networks During Precise Grasping

Zhixian Gao, Shiyang Lv, Xiangying Ran, Mengsheng Xia, Mengyue Qiu, Junming Wang, Yinping Wei, Zhenpeng Shao, Xuezhi Zhou, Yehong Zhang, Zongya Zhao, and Yi Yu

***Abstract*— Visual feedback gain is a crucial factor influencing the performance of precision grasping tasks, involving multiple brain regions of the visual motor system during task execution. However, the dynamic changes in brain network during this process remain unclear. The aim of this study is to investigate the impact of changes in visual feedback gain during precision grasping on brain network dynamics. Sixteen participants performed precision grip tasks at 15% of MVC under low (0.1°), medium (1°), and high (3°) visual feedback gain conditions, with simultaneous recording of EEG and right-hand precision grip data during the tasks. Utilizing electroencephalogram (EEG) microstate analysis, multiple parameters (Duration, Occurrence, Coverage, Transition probability(TP)) were extracted to assess changes in brain network dynamics. Precision grip accuracy and stability were evaluated using root mean square error(RMSE) and coefficient of variation(CV) of grip force. Compared to low visual feedback gain, under medium/high gain, the Duration, Occurrence, and Coverage of microstates B and D increase, while those of microstates A and C decrease. The Transition probability from microstates A, C, and D to B all increase. Additionally, RMSE and CV of grip force decrease. Occurrence and Coverage of microstates B and C are negatively correlated with RMSE and CV. These findings suggest that visual feedback gain affects the brain network dynamics during precision grasping; moderate increase in visual feedback gain can enhance the accuracy and stability of grip force, whereby the increased Occurrence and Coverage of microstates B and C contribute to improved performance in precision grasping. Our results play a crucial role in better understanding the impact of visual feedback gain on the motor control of precision grasping.**

***Index Terms*— EEG, microstate, visual feedback gain, precise grasping, brain network dynamics.**

I. Introduction

DURING motor execution, the brain continuously compares incoming sensory signals with predicted sensory outcomes to adaptively guide and correct movements [1]. In the process, visual feedback is a key source of information for achieving precise motor control [2], which allows performers to obtain information about the effectiveness of movement execution by observing their own movements or changes in the environment, which is crucial for the accuracy, coordination, and adaptability of motor control. An important parameter affecting motor performance through visual feedback is the gain of visual feedback, initially introduced into the study of motor control by [3]. As the visual feedback gain increases, the spatial amplitude of the visual stimulus increases, and more details of movement execution outcomes are captured by the visual system. This enhanced visual information input can activate the human visual cortex, enhancing visual sensation and processing abilities [4]. Subsequently, abundant visual motion information is projected to brain cortical areas related to movement, integrated to optimize movement planning and execution, thereby enhancing motor performance [5], [6]. Studies have shown that the gain of visual feedback is closely related to motor performance, and increasing the gain of visual feedback within a certain range can reduce movement errors and variability, thereby improving motor performance [7], [8].

Manuscript received 15 April 2024; revised 1 July 2024; accepted 31 July 2024. Date of publication 5 August 2024; date of current version 12 August 2024. This work was supported in part by the Innovative Research Team (in Science and Technology) in University of Henan Province under Grant 24IRTSTHN042, in part by the Major Science and Technology Projects of Henan Province under Grant 221100310500, in part by the National Natural Science Foundation of China under Grant 82201709 and Grant 82302298, in part by the Science and Technology Research Project of Henan Province under Grant 242102310055 and Grant 242102310005, and in part by the Open Project Program of Henan Collaborative Innovation Center of Prevention and Treatment of Mental Disorder under Grant XTkf07. *(Zhixian Gao, Shiyang Lv, and Xiangying Ran are co-first authors.) (Corresponding authors: Zhixian Gao; Yi Yu; Zongya Zhao.)*

This work involved human subjects or animals in its research. Approval of all ethical and experimental procedures and protocols was granted by the Ethics Committee of Xinxiang Medical University under Approval No. XYLL20230015, and performed in line with the Declaration of Helsinki.

The authors are with the School of Medical Engineering, Xinxiang Medical University, Xinxiang 453004, China, also with the Engineering Technology Research Center of Neurosense and Control of Henan Province, Xinxiang 453004, China, and also with Henan International Joint Laboratory of Neural Information Analysis and Drug Intelligent Design, Xinxiang 453004, China (e-mail: gaozhixian@xxmu.edu.cn; zhaozongya_paper@126.com; yuyi@xxmu.edu.cn).

This article has supplementary downloadable material available at https://doi.org/10.1109/TNSRE.2024.3438674, provided by the authors.

Digital Object Identifier 10.1109/TNSRE.2024.3438674

© 2024 The Authors. This work is licensed under a Creative Commons Attribution 4.0 License.
For more information, see https://creativecommons.org/licenses/by/4.0/

Neuroimaging studies have demonstrated that the improvement in motor performance relies on the integrated network of the brain's visual motor system, including the visual cortex, parietal cortex, motor cortex, premotor cortex, supplemental motor area, and cerebellum [9], [10]. [11] recorded electroencephalogram (EEG) signals during precise grasping tasks under varying visual feedback gains and found that as the visual feedback gain increased, task performance significantly improved. Moreover, under higher visual feedback gains, there was an increase in theta synchronization in the midfrontal area and enhanced beta desynchronization in the sensorimotor and posterior parietal areas. Reference [12] utilized functional magnetic resonance imaging (fMRI) and found that with increasing visual feedback gains, the mean force error decreased, accompanied by increased BOLD signal activity in the primary motor cortex, premotor cortex, parietal cortex, extrastriate visual cortex, basal ganglia, and cerebellum [11], [12]. Researchs exploring the impact of visual feedback gains on brain activity during precise grasping are primarily focused on specific brain areas or frequency bands, with a priori hypotheses [13]. However, precise grasping tasks under visual feedback involve multiple brain regions, necessitating a global perspective on the brain, abandoning a priori hypotheses, and considering the global response of brain network dynamics.

The EEG microstate analysis method captures EEG signals from all channels simultaneously, computes global representations of brain functional states, and investigates dynamic changes in brain functional networks at the millisecond time scale, offering high temporal resolution and reliability [14]. Microstates that remain relatively stable and quickly transition within a certain period represent the brain's response to stimuli and information processing, reflecting dynamic changes in brain networks [15]. Previous studies have utilized methods such as simultaneous EEG-fMRI [16] or EEG source localization [17] to explore the relationship between EEG microstate and resting-state brain networks: Microstate A is associated with activation of the auditory network; Microstate B is related to activity in visual areas; Microstate C is linked to the default mode network (DMN); Microstate D is associated with the dorsal attention network (DAN) and the executive control network (ECN) [18], [19], [20]. In recent years, researchers have applied EEG microstate to task-related studies. Reference [21] found 4 microstates under both sustained grasping and resting conditions, with highly consistent topographic maps of three microstate (B, C, and D) across the two conditions. Reference [22] found that the parameter of microstate C changed significantly with the increase in grip force level. These results indicate that EEG microstate analysis can be used to investigate the dynamic changes in brain networks when control conditions change during grip tasks, providing a powerful tool for studying the impact of visual feedback gain on the dynamics of brain networks during precision grasping.

The aim of this study is to investigate the impact of changes in visual feedback gain during precision grasping on the dynamics of brain networks using EEG microstate analysis. To achieve this, we recorded the mechanics and EEG signals during precision grip tasks under different visual feedback gains (low, medium, high), and reported the changes in precision grip performance and EEG microstate, as well as their correlation. We hypothesize that with the increase in visual feedback gain, grip accuracy and stability will improve, leading to a significant enhancement in motor performance. At the same time, EEG microstate parameters will undergo significant changes. To our knowledge, this is the first study to investigate the impact of visual feedback gain on the dynamics of brain networks during precision grasping using EEG microstate.

II. Method

A. Subjects

Sixteen graduate/undergraduate students (7 males, mean age 20.4 ± 2.2 years) voluntarily participated in this study. All participants had no history of orthopedic, neurological, or cognitive disorders that could affect task performance, and had normal or corrected-to-normal vision. Before the formal experiment, all participants were given sufficient rest and underwent state adjustments to avoid fatigue or psychological factors that could interfere with the experimental tasks. The Edinburgh Handedness Inventory was used to ensure that all participants were right-handed [23]. This study was approved by the Ethics Committee of Xinxiang Medical University(XYLL20230015) and conducted in accordance with the Helsinki Declaration, with all participants providing written informed consent.

B. Experimental Paradigm

Participants sat on a chair with a backrest, maintaining a specific posture: upright sitting position, shoulder joints abducted by 30°, elbow joints flexed by 90°, forearms placed horizontally on the table, and right hand grasping a cylindrical grip force sensor. A screen was placed 60 cm away from the participants' eyes. To avoid environmental distractions around the screen, the room lights were turned off, creating dim lighting around the screen (**Figure 1a**).

To determine the maximum voluntary contraction (MVC) grip strength, participants were instructed to generate maximum grip force within 5 seconds, with verbal encouragement provided. The average of three trials of maximum grip strength was set as MVC. To prevent muscle fatigue, a 60-second rest was given between each attempt. In this study, 15% of MVC was set as the target grip strength. The screen displayed a target line (red/green) and a real-time grip force line (white). To ensure accurate viewing angle, the target line remained at the center of the screen, while the grip force line moved relative to grip force changes. Each trial of the precision grip tracking task comprised four stages (**Figure 1b, c**): Rest (10s) - the target line was red, and no grip force was applied; Up (4s) - the target line turned green, indicating gradual force application to avoid large fluctuations during initial force application; Constant (10s) - participants aimed to align the grip force line with the target line as closely as possible; Down (2s) - gradually reducing the grip force to zero. Participants performed a total of 10 trials under a visual feedback gain. Participants were instructed to minimize head and body movements during the task to reduce motion artifacts and electromyographic interference. Prior to the formal experiment, participants are required to undergo at

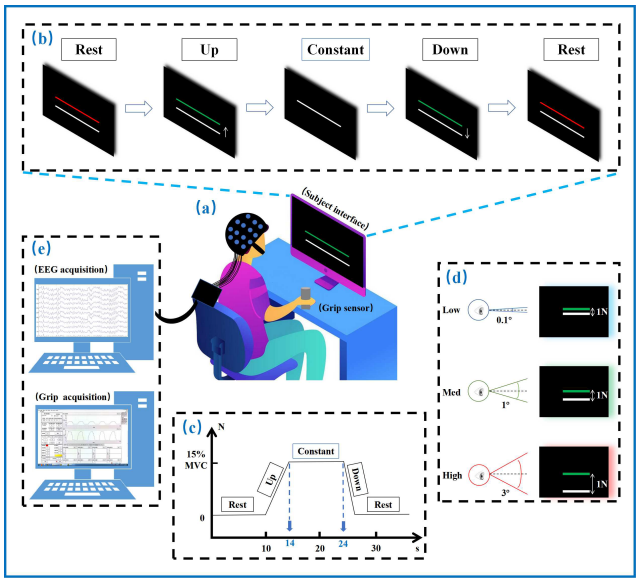

Fig. 1. Experimental Setup and Data Acquisition Diagram. **(a) Experimental setup:** Participants hold the grip force sensor in the prescribed posture and perform precise grip force tracking tasks with visual feedback from the screen. **(b) Grip force tracking diagram:** The four stages of the precise grip force tracking task: Rest, Rise, Sustain, and Descend. The red line indicates rest, the green line indicates the application of grip force, and the white line represents real-time grip force. **(c) Grip force trajectory diagram:** The grip force trajectory formed during one trial, observed only by the experimenter on the monitoring screen. **(d) Conceptual diagram of visual feedback gain:** As the visual feedback gain increases, the displacement variation displayed on the screen increases. **(e) Data acquisition:** Participant's EEG and grip force data are collected separately through EEG acquisition system and LabVIEW system.

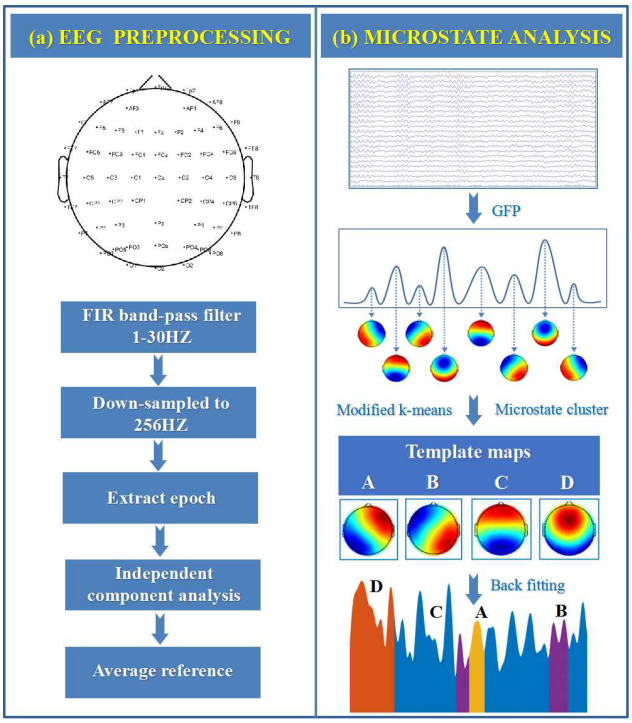

Fig. 2. Flow chart of EEG preprocessing and microstate analysis. **(a) EEG preprocessing**. **(b) Microstate analysis.**

least four trials until they understand and can independently complete the tasks without verbal prompts.

Three visual feedback conditions were selected: 0.1°, 1°, and 3° angles representing low, medium, and high feedback gains, respectively (**Figure 1d**). Visual feedback gain was manipulated by varying the amplitude of grip force fluctuations on the screen, implemented using Equation (1) [24]:

$$\alpha = 2\tan^{-1}\left(\frac{H_1}{D}\right). \tag{1}$$

Here, H_1represents half of the amplitude of force fluctuations displayed on the screen, D denotes the distance from the subject's eyes to the screen, and α stands for the human eye's visual angle. According to previous studies [12], [25], [26], the standard deviation of force output was estimated to be 0.3 N, and this value was multiplied by 6 to approximate the full range of force fluctuations (±3SD), thus yielding H_1 as 3SD. However, the results of the aforementioned studies were based on pinch force tasks, whereas the current study focused on grip force tasks. Therefore, we compared the differences in standard deviations (SDs) between pinch and grip forces at the same force levels and found that the grip force SD was approximately four times greater than that of pinch force (see **Supplementary Material** for details).

C. Data Acquisition

EEG signals during the task were recorded using a 64-channel electroencephalography (EEG) acquisition system (NeuSen W, neuracle, China) (**Figure 1e**). Electrode impedance was adjusted to below 10 $k\Omega$, with a sampling rate of 1000 Hz, and offline saved for subsequent processing.

Grip force data from participants were collected using a cylindrical mechanical sensor with a resolution of 0.025 N (**Figure 1e**). The force signals were transmitted via optical fiber cables to an NI USB-6210 data acquisition card, with a sampling rate of 1000 Hz, and displayed and saved in the LabVIEW system.

D. Data Preprocessing

Standard preprocessing of EEG data collected (Figure 2a) was conducted. Firstly, electrode channel localization was performed to match the recorded EEG data with channel position information. Secondly, redundant electrodes, including ECG, HEOR, HEOL, VEOU, and VEOL, were removed. Thirdly, EEG data were bandpass filtered between 1-30 Hz [27], and a 50 Hz notch filter was applied to eliminate power line interference. Fourthly, the EEG sampling rate was reduced to 256 Hz to reduce data volume and enhance computational speed. Fifthly, segments containing only EEG data during the sustained force phase (10s) were extracted. Sixthly, independent component analysis (ICA) was performed to eliminate artifacts caused by eye, cardiac, and muscle activities, with manual inspection for further exclusion. Finally, EEG data were re-referenced to a spatial zero-mean distribution.

Grip force data were filtered using a 20 Hz low-pass filter to remove artifacts and extract grip force data during the sustained force phase for analysis.

E. Data Analysis

1) EEG Microstate Analysis: The study found that EEG data lasting 90-120 seconds demonstrates high reliability in

microstate analysis [28]. In our study, each participant's EEG data during the sustained force phase under one visual feedback gain condition, totaling 100 seconds (10s * 10 trials), were analyzed. Microstate analysis was conducted using the microstate analysis toolbox based on the EEGLAB toolbox [29]. The analysis process comprised four key steps (Figure 2b). Firstly, the global field power (GFP) of EEG signals at a certain moment was calculated based on the potential values of individual electrode channels of each participant. The definition of GFP is shown in Equation (2).

$$GFP = \sqrt{\frac{\sum_{i=1}^{n} u_i^2}{n}}. \tag{2}$$

Here, i represents each electrode, n denotes the total number of electrodes, and u represents the measured voltage of each channel. Further, the time series of maximum GFP values are extracted. In the second step, the improved k-means clustering algorithm [30] is applied to cluster the time series of maximum GFP values for each participant. We set the number of clusters to range from 3 to 8 and employed the KL cross-validation criterion [30], resulting in the optimal number of clusters being 4. Subsequently, the program randomly selects four brain topographies as initial cluster centers. It then compares the remaining topographic maps with these initial cluster centers and labels the topographic maps most related to each initial cluster center. New cluster centers are calculated, and this process is repeated until the percentage of all EEG signals represented by the cluster centers no longer improves. The four cluster centers obtained at this point are referred to as the "template maps" [29]. In the third step, the "template maps" for each visual feedback gain condition are computed based on all participants' data, resulting in four categories of brain topographies labeled as microstate A, B, C, and D within the group. In the fourth step, spatial correlation is utilized to fit the four categories of "template maps" and the original EEG data. Each time point of the original EEG data is labeled with the microstate showing the highest correlation, resulting in the temporal evolution of brain topographies. Subsequently, microstate feature parameters are further extracted for analysis.

For each participant under each visual feedback gain condition, we calculated the following features of EEG microstate:

(a) Duration: The average duration of maintaining a stable state when a certain microstate appears, reflecting the stability of underlying neural components.

(b) Occurrence: The average number of occurrences of a certain microstate per second, reflecting the trend of activation of potential neural generators.

(c) Coverage: The time coverage of a certain microstate during the total analysis time, reflecting the relative time coverage of underlying neural generators compared to others.

(d) Transition Probability (TP): The probability of transition from one microstate to another. For example, the transition probability from microstate A to microstate B is defined as the number of transitions from A to B divided by the total number of transitions from A to the other three microstate [31]. It reflects the sequential activation of neural networks.

2) Grip Strength Data Analysis: To assess grip performance, we computed the root mean square error (RMSE) and coefficient of variation (CV) of real-time grip force. RMSE is used to measure the deviation between observed values and true values, reflecting the accuracy of grip force. CV is used to measure the dispersion of data, reflecting the stability of grip force. Their definitions are shown in equations (3) and (4):

$$RMSE = \sqrt{\frac{\sum_{i=1}^{n} \left(X_{obs,i} - X_{\text{model},i}\right)^2}{n}}. \tag{3}$$

where, $X_{obs,i}$ is the observed value of the sample, and $X_{model,i}$ is the simulated value (true value) of the sample.

$$C_v = \frac{\sigma}{\mu}. \tag{4}$$

where, σ is the sample standard deviation and μ is the sample mean.

F. Statistical Analysis

This study employed the Ragu toolbox [32] for Topographic Analysis of Variance (TANOVA) to investigate whether there were statistical differences in microstate topographies among conditions. Statistical analysis was performed using SPSS19. The Shapiro-Wilk test was used to assess the normality of the data, and all data met or approximately met the normal distribution. One-way repeated measures analysis of variance (ANOVA) was conducted to assess the between-group differences in microstate parameters (Duration, Occurrence, Coverage, TP) and grip force parameters (RMSE, CV), with a significance level set at 0.05 and Bonferroni correction applied to control for multiple comparisons. To quantify the relationship, Pearson correlation tests were conducted between microstate parameters and mechanical parameters under each visual feedback gain. False Discovery Rate (FDR) correction was applied for multiple comparisons of p-values, with a significance level set at 0.05 for correlation.

III. Result

A. EEG Microstate Topographic Map

According to the improved k-means clustering algorithm and KL cross-validation criteria, the optimal number of microstate under low, medium, and high visual feedback gain conditions was 4, namely A, B, C, and D. As shown in Figure 3, the obtained four microstate topographies were similar to the classical microstate topographies reported previously [33], [34], with microstate A showing a left posterior to right anterior pattern, microstate B showing a right posterior to left anterior pattern, microstate C showing a symmetric distribution between the two hemispheres, from occipital to frontal regions, and microstate D showing frontal-central activity. No inter-group differences in microstate topographies were found using TANOVA ($P > .05$). To evaluate the extent to which microstates explain the original EEG data, the Global Explained Variance (GEV) for the Low, Med, and High groups were 75.1±4%, 71.2±4%, and 70.4±3%, respectively. No significant differences were found for microstate GEV($P > .05$).

TABLE I

STATISTICAL COMPARISON OF PARAMETERS (DURATION, OCCURRENCE, COVERAGE) FOR THE SAME MICROSTATE UNDER DIFFERENT VISUAL FEEDBACK GAIN CONDITIONS

	Mean per gain(mean±sd)			$P_{Bonferroni}$		
	Low	Med	High	Low vs. Med	Low vs. High	Med vs. High
Duration(ms)						
A	91.72±15.30	68.37±5.12	67.88±7.01	< **.001**	< **.001**	> 0.999
B	89.66±10.11	129.0±13.14	130.99±17.33	< **.001**	< **.001**	0.808
C	121.70±17.06	94.59±8.75	99.04±12.83	< **.001**	< **.001**	0.063
D	79.42±6.15	84.94±7.07	84.25±7.24	**0.015**	**0.022**	> 0.999
Occurencce(Hz)						
A	2.40±0.32	1.42±0.16	1.36±0.21	< **.001**	< **.001**	0.641
B	2.42±0.31	3.43±0.42	3.43±0.51	< **.001**	< **.001**	> 0.999
C	3.35±0.5	2.74±0.36	2.78±0.43	< **.001**	< **.001**	> 0.999
D	2.11±0.3	2.47±0.17	2.34±0.22	**0.001**	**0.038**	0.101
Coverage(%)						
A	21.7±3.07	9.7±1.37	9.2±1.72	< **.001**	< **.001**	0.819
B	21.5±2.29	43.7±1.07	44.1±1.14	< **.001**	< **.001**	0.723
C	40.0±1.98	25.7±2.16	27.1±2.04	< **.001**	< **.001**	0.082
D	16.8±2.53	20.9±2.15	19.7±2.04	**0.001**	**0.003**	0.136

TABLE II

COMPARISON OF TP DIFFERENCES UNDER DIFFERENT VISUAL FEEDBACK GAINS

Transitions(%)	Mean per gain(mean±sd)			$P_{Bonferroni}$		
	Low	Med	High	Low vs. Med	Low vs. High	Med vs. High
B→A	26.13±5.88	18.69±3.42	18.65±2.92	**0.001**	**0.001**	> 0.999
C→A	35.31±5.05	17.63±4.47	15.66±4.20	< **.001**	< **.001**	0.367
D→A	28.03±3.67	12.61±2.75	12.46±3.88	< **.001**	< **.001**	> 0.999
A→B	25.18±5.07	45.81±6.66	48.39±4.84	< **.001**	< **.001**	0.520
C→B	35.56±4.72	53.66±7.67	55.73±6.66	< **.001**	< **.001**	0.568
D→B	29.98±5.25	52.37±5.83	51.25±4.35	< **.001**	< **.001**	> 0.999
A→C	51.90±5.72	34.45±6.59	33.64±5.47	< **.001**	< **.001**	> 0.999
B→C	50.03±7.54	39.94±5.53	42.61±6.21	< **.001**	**0.018**	0.209
D→C	41.99±6.41	35.02±5.48	36.29±5.16	**0.023**	0.061	> 0.999
A→D	22.92±3.15	19.74±4.81	17.97±4.41	0.255	**0.005**	0.833
B→D	23.84±5.15	41.37±3.6	38.74±4.81	< **.001**	< **.001**	0.078
C→D	29.13±5.35	28.71±4.51	28.61±4.75	> 0.999	> 0.999	> 0.999

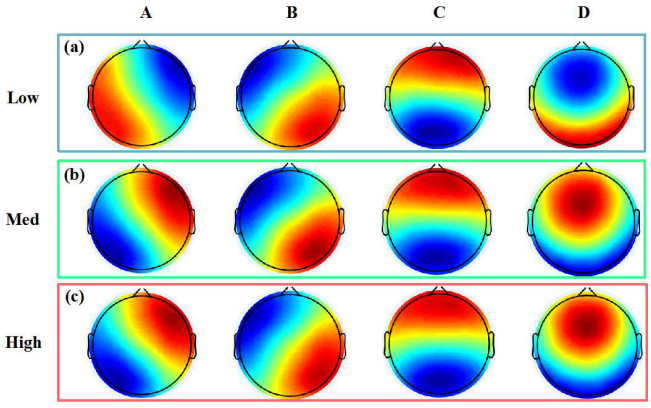

Fig. 3. The topographies of EEG microstate under low (a), medium (b), and high (c) visual feedback gain conditions. Microstate A, B, C, and D are arranged from left to right.

B. EEG Microstate Parameters

The metrics of Duration, Occurrence, Coverage, and TP of EEG microstate were extracted to investigate the differences in brain network dynamics under different visual feedback gain conditions. The results revealed that, compared to the low visual feedback gain condition, the Duration of microstate B and D significantly increased under medium/high gains, while the Duration of microstate A and C decreased significantly. There were no significant differences in the Duration of microstate A, B, C, and D between medium and high visual feedback gain conditions (**Figure 4a**). Occurrence (**Figure 4b**) and Coverage (**Figure 4c**) exhibited similar trends. The specific statistical results are shown in **Table I**. However, although the parameter values of microstate C decreased under medium/high visual feedback gains, they remained significantly higher than those of microstate A and D under each visual feedback gain condition (**Figure 5**). The above results suggest that microstate B and C may still play a positive role in visual motion.

The results of TP are shown in **Figure 6**. Compared to low visual feedback gain, in medium/high gain conditions, the TP from microstate A, C, and D to B significantly increased, while the TP from other microstate to A/C significantly decreased. Meanwhile, the TP from microstate B to D significantly increased. The specific statistical results are shown in Table II. Additionally, under low visual feedback gain, the proportion of TP to microstate C was the highest, reaching 143.92%, while the proportions of TP to microstate A, B, and D were relatively low, at 89.47%, 90.72%, and 75.89%, respectively (**Figure 6b**). Compared to low visual feedback gain, in medium/high gain conditions, the proportion of TP to microstate B significantly increased, rising to 151.84% and 155.37%, respectively; the proportion of TP to microstate D slightly increased, reaching 89.82% and 85.32%, respectively; whereas the proportion of TP to

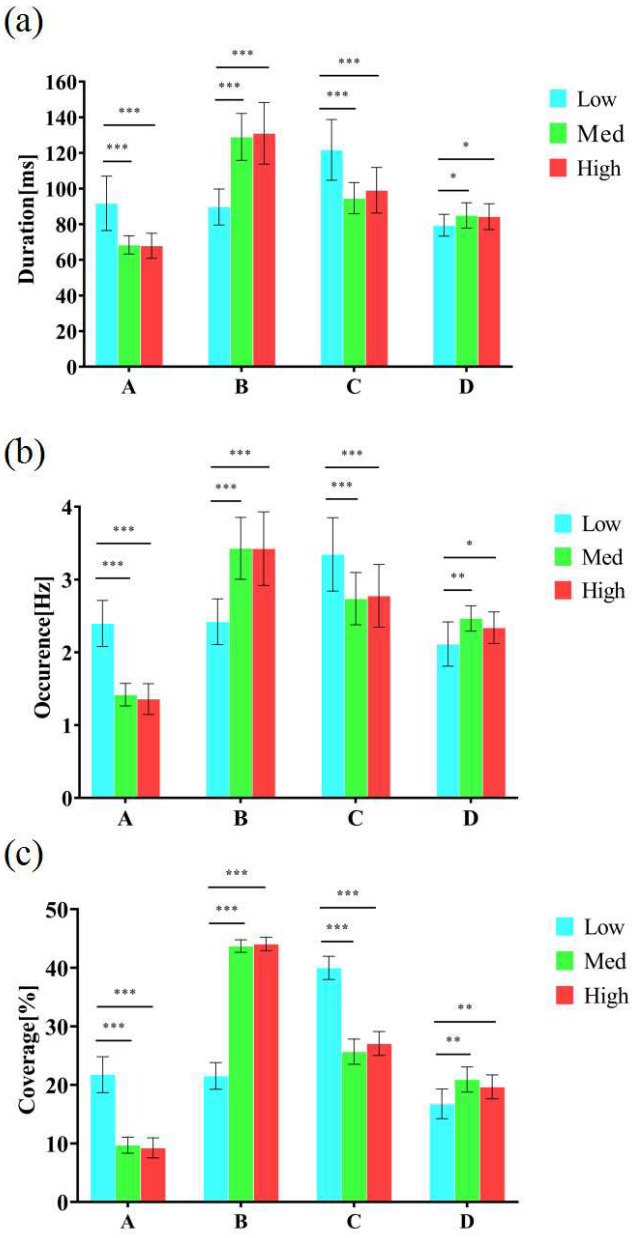

Fig. 4. The comparison of parameters for the same microstate under different visual feedback gain conditions: **(a) Duration**,**(b) Occurrence**, and **(c) Coverage**.

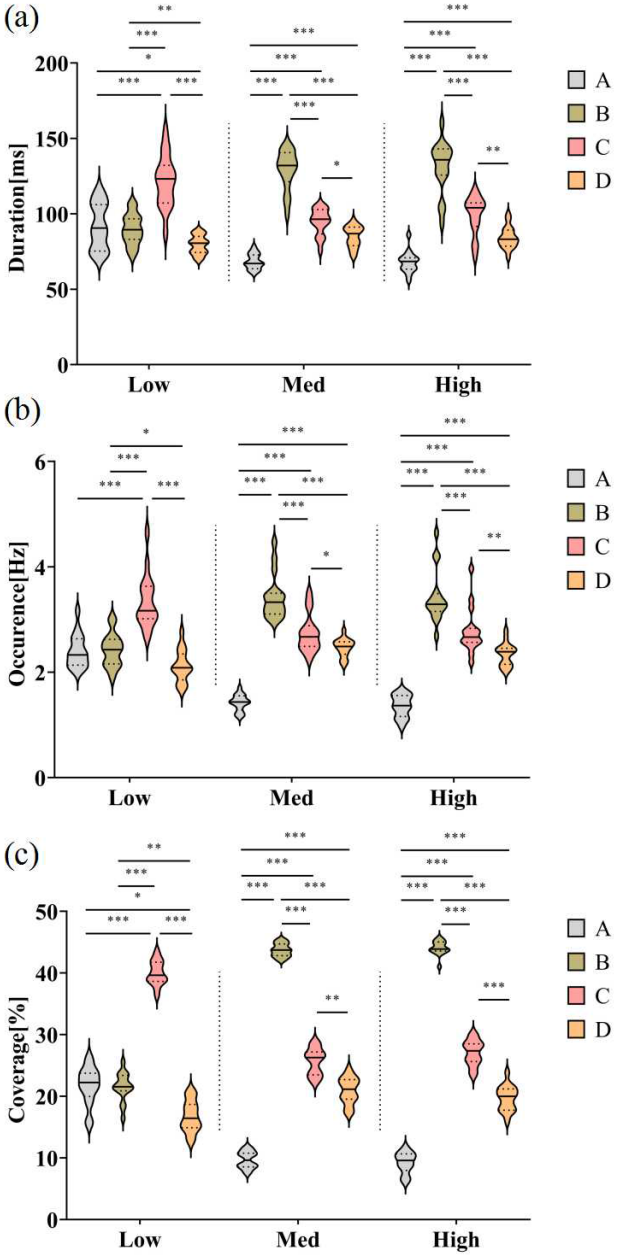

Fig. 5. The comparison of parameters for different microstate under the same visual feedback gain condition: **(a) Duration**,**(b) Occurrence**, and **(c) Coverage**.

microstate A significantly decreased, dropping to 48.93% and 46.77%, respectively; the proportion of TP to microstate C also notably decreased, declining to 109.41% and 112.54%, respectively (**Figures 6c, d**). However, we observed a phenomenon similar to **Figure 4**: compared to low visual feedback gain, under medium/high visual feedback gain conditions, the TP from other microstate to C decreased (**Figure 6**), but the proportion of TP tao microstate C remained higher than that to microstate A and D (**Figures 6c, d**). This result once again indicates the potentially important role of microstate B and C in visual motion.

C. Grip Performance

We analyzed grip parameters, including RMSE and CV, to assess the impact of visual feedback gain on grip accuracy and stability. The results revealed a significant decrease in RMSE with increasing visual feedback gain (**Figure 7a**). The CV under medium/high visual feedback gain was significantly lower than that under low visual gain, with no significant difference between medium and high visual feedback gains (**Figure 7b**). This indicates that increasing visual feedback gain can significantly improve grip accuracy. Grip stability was significantly higher under medium/high visual feedback gain compared to low visual feedback gain.

D. Correlation Between Microstate and Grip Strength Parameters

It was found from the above results that microstate B and C may play a positive and crucial role in visual motor tasks. Therefore, we conducted Pearson correlation analyses between

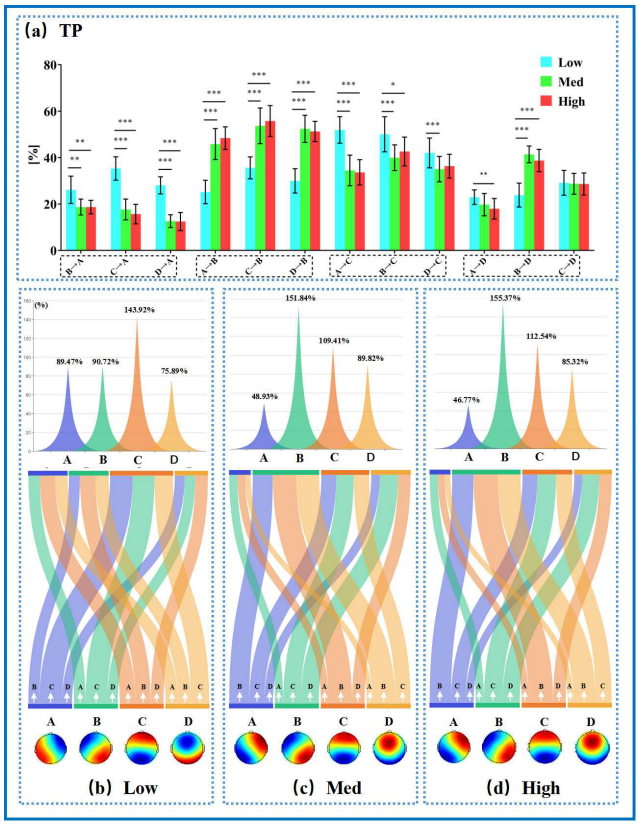

Fig. 6. Microstate TP and flow proportion under low, medium, and high visual feedback gain conditions. (a) Statistical analysis of microstate TP differences under different visual feedback gain conditions. Flow direction and proportion of TP under low (b), medium (c), and high (d) visual feedback gain conditions.

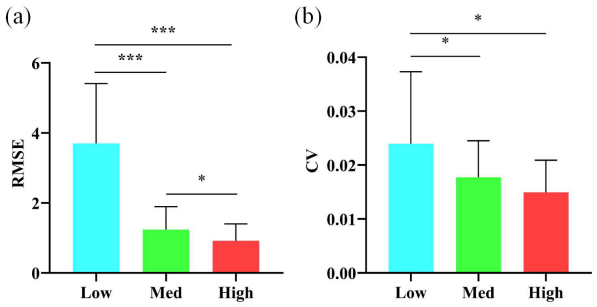

Fig. 7. Grip parameters RMSE(a) and CV(b) under different visual feedback gain conditions.

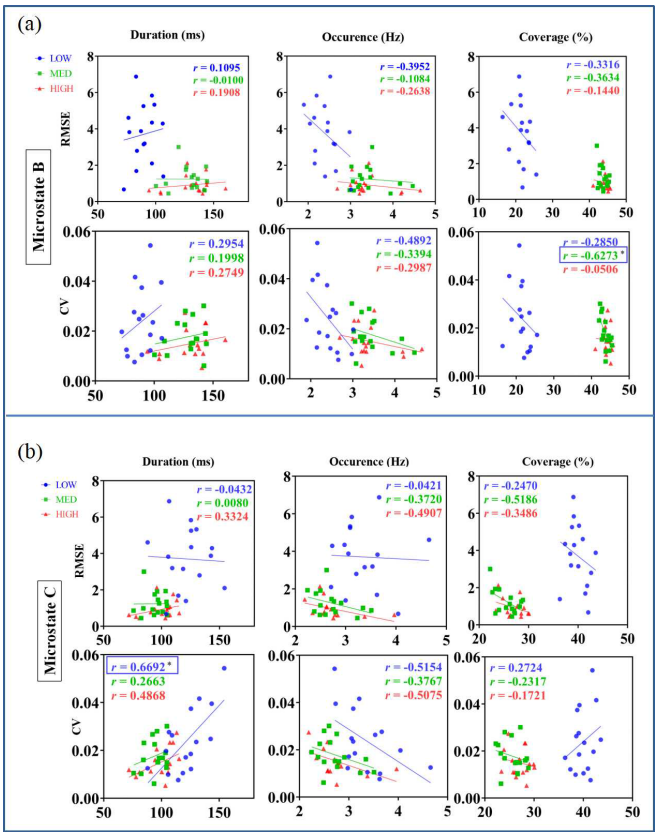

Fig. 8. Correlation between microstate and grip parameters. (a) Correlation of microstate B parameter with RMSE and CV. (b) Correlation of microstate C parameter with RMSE and CV.

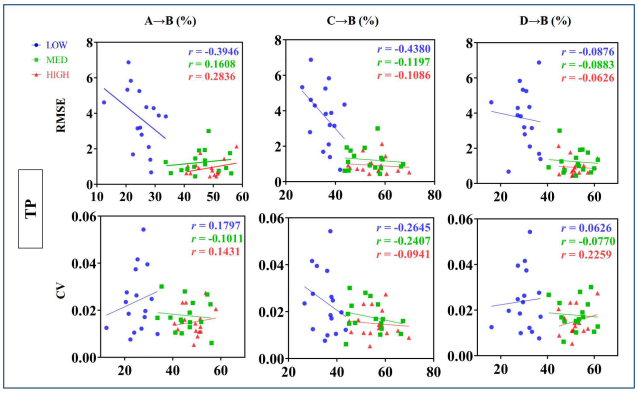

Fig. 9. The correlation between TP to microstate B and RMSE, as well as CV.

microstate B and C parameters and grip parameters under each visual feedback gain condition (**Figure 8**). The results revealed a negative correlation between the Occurrence and Coverage of microstate B and C and RMSE, as well as CV. Specifically, under medium visual feedback gain, the Coverage of microstate B showed a significant negative correlation with CV ($R = -0.6273$, $P_{FDR} = 0.0279$). This suggests that as the Occurrence and Coverage of microstate B and C increase, RMSE and CV decrease, indicating a positive effect on the accuracy and stability of precise grip force.

However, under all three gain conditions, the Duration of microstate B and C shows predominantly positive correlations with RMSE and CV. Specifically, under low visual feedback gain, the Duration of microstate C shows a significant positive correlation with CV ($R = 0.6692$, $P_{FDR} = 0.0138$). These results suggest that the longer the Duration of microstate, the poorer the accuracy and stability of grip force, which may be less favorable for improving motor performance.

As the TP from microstate A, C, and D to B significantly increases under medium/high visual feedback gain, we further analyzed the correlation between the TP from other microstate to B and precise grip force parameters (**Figure 9**). The results revealed a negative correlation between the TP from microstate C to B and RMSE, as well as CV. This indicates that the transition from microstate C to B may contribute to improving grip performance.

IV. Discussion

To investigate the impact of visual feedback gain on the dynamics of brain networks during precise grasping,

we utilized the emerging neuroimaging method of EEG microstate to analyze the performance of precise grip and the changes in microstate under low, medium, and high visual feedback gains.

In this study, increasing visual feedback gain actually enhanced the stimulating effect of precise grip force variation. Although the absolute force output of precise grip is the same (15% MVC), the different visual feedback gains in fact artificially increase the resolution of force variation under medium/high visual feedback gain conditions, amplifying the error of precise grip force output, allowing subjects to see more details of force output for precise dynamic adjustments. Therefore, under medium/high visual feedback gain conditions, the RMSE and CV of precise grip are significantly lower, and motor performance is significantly improved.Meanwhile, under medium/high visual feedback gain conditions, there are significant changes in EEG microstate, with significant increases in parameters of microstate B and D, significant decreases in parameters of microstate A and C, and significant increases in transitions to microstate B. This indicates that visual feedback gain may improve precise grip control through dynamic adjustments to brain networks.

A. The Visual Feedback Gain Affects the Microstate Parameters

For the parameters of microstate B, we found that under medium/high gain, the Duration, Occurrence, and Coverage of this microstate were significantly higher than those under low gain. This is consistent with the findings of [35], who found a significant increase in the Duration and Coverage of microstate B during a visual task involving maintaining the orientation of objects in space. Microstate B is believed to be associated with vision, with its neural generators originating from the occipital lobe's visual network, involving visual spatial attention and processing [16], [17], [18], [19]. In our visual motion task, as the visual feedback gain increases, the human eye can observe more subtle motion information, more visual information is captured, the processing capacity of the visual network is enhanced, thus the microstate B reflecting the brain's visual spatial attention and processing capacity becomes more active. Similar results have been reported in other studies employing visual-related paradigms, where the Occurrence and Coverage of microstate B significantly increased after visual stimulation or during open-eye states compared to resting-state or closed-eye conditions [36], [37].

Parameters of microstate C are significantly lower under medium and high visual feedback gain conditions compared to low visual feedback gain. This may be because microstate C is believed to be associated with the DMN [18], [19], [38]. DMN is a task-negative network, meaning it is activated when the brain is in a wakeful resting state but attenuated during externally goal-directed tasks [39], [40]. In this study, as the visual feedback gain increases, task intensity rises, brain activity enhances, and microstate C is suppressed. Reference [35] similarly found a significant decrease in the Duration and Coverage of microstate C during a visual spatial motion task. However, interestingly, microstate C parameter values remain higher than A and D at medium/high gain. This may be because the DMN serves as the central hub of brain organization and function, playing a fundamental role in brain function [41], and it always starts from a highly active baseline, making minimal adjustments during activity to accommodate the demands of specific tasks [42].

Microstate D exhibits a trend like microstate B, with its parameters significantly increasing under medium/high visual gain. Reference [13] found that in visually feedback-controlled finger pinch force, the Duration and Occurrence of microstate D significantly increase compared to the resting state. Microstate D is believed to be associated with DAN and ECN [16], [17], [18], [19], [38]. With the increase in visual feedback gain, more motor stimuli are projected to the motor-related cortex for frequent integration and optimization, enhancing the interaction between the brain and the peripheral environment, thus making microstate D, reflecting the attention and executive control abilities of the brain, more active. We found that microstate A parameters are like those of microstate C. Reference [43] made a similar discovery, observing a decrease in the Duration of microstate A under open-eye conditions compared to closed-eye conditions. Considering that microstate A is associated with the auditory network [16], [17], [18], [19], with its neural generator originating from the temporal lobe cortex, in visual motor tasks unrelated to auditory information, microstate A may be suppressed by the brain's cognitive control capacity to prioritize resource allocation for task-related information processing [44].

TP between microstate provides information on the overall temporal sequence and network dominance. Our results revealed TP from other microstate to B significantly increased under medium/high gain. Moreover, there was a significant mutual increase in TP between microstate B and D. Visual motion involves a complex dynamic closed-loop mechanism [45]: integration of perception and decision-making, movement planning and execution, feedback, and adjustment. Therefore, the increased TP between microstate B and D may reflect the frequent alternation of corresponding functional networks [46], to adapt to task requirements and achieve precise and coordinated motion control. This suggests that the visual network, DAN and ECN play a key role in visual-motion integration [13].

B. Relationship Between Grip Performance and Microstate B, C Parameters

As microstate B and C may play crucial roles in visual motion, we conducted a correlation analysis between their parameters and RMSE, CV. The results revealed Occurrence and Coverage of microstate B and C are negatively correlated with RMSE and CV, indicating their positive impact on visual motion performance. In our motor paradigm, the visual network plays a crucial role. With the increase of gain, the functionality of the visual network strengthens, microstate B becomes more active, and both grip accuracy and stability significantly improve. Although microstate C represents a task-negative network and is suppressed during task execution, it still plays a fundamental role as a hub of brain structure and function [41]. Therefore, microstate C occupies a crucial position under medium/high gain, as reflected in TP. TP towards

microstate C is significantly higher than towards A and D, and TP from microstate C to B is negatively correlated with RMSE and CV, indicating that microstate C contributes to improved motor performance.

However, the Duration of microstate B and C mostly shows a positive correlation with RMSE and CV, indicating that the longer the average Duration of maintaining stable states when microstate occur, the worse the grip performance. A plausible explanation might be that visual motion involves complex dynamic adjustment mechanisms [45], requiring coordinated activation among various brain networks for dynamic alternation. If certain functional networks remain continuously activated, indicating the persistent existence of microstate representing these networks, it may interfere with the dynamic adjustment mechanisms of various networks during visual motion [47], [48], thereby impeding the improvement of motor performance.

C. The Dynamic Response of Brain Networks Is Constrained as Visual Feedback Gain Increases

It is worth noting that there were no significant differences in the parameters of each microstate between the medium/high gain ((**Figure 4**)), a phenomenon also observed in CV (**Figure 7b**). One possible explanation is that brain resources are limited. Within a certain range of gains, as visual feedback gain increases, the dynamic response of brain networks significantly improves, enhancing activation of the visual motor system [12], enabling better completion of tasks, and improving grip stability. However, beyond this range, an excessive amount of visual motion information imposes a heavy burden on the reception and processing of the brain's visual motor system, limiting the dynamic response of brain networks, and grip stability no longer improves. This suggests that grip stability may depend more on the dynamic response of brain networks.

D. Limitations and the Future directions

While the current study presents significant findings, several limitations need to be acknowledged and addressed in future research. Firstly, the current study only analyzed brain network dynamics and precise grip performance at three visual angles: 0.1° (Low), 1° (Med), and 3° (High). However, previous research found that when the visual angle is $<1°$, small changes in the spatial amplitude of visual feedback are accompanied by a substantial reduction in force error, while at visual angles $>1°$, large changes in the spatial amplitude of visual feedback result in a slight reduction or no improvement in force error [12]. Therefore, future studies should categorize visual angles into more levels to further investigate the broad impact of visual feedback gain on brain network dynamics. Secondly, the EEG data used in this study lasted for 100 seconds, which has high reliability in EEG microstate analysis [28]. However, using longer task durations in the future could further validate the robustness of the results. Finally, the current study relies solely on EEG signals, which may not comprehensively capture our findings. Future research should incorporate fMRI and source localization techniques to gain a deeper understanding of the brain networks represented by each microstate [16], [17].

V. Conclusion

To investigate the impact of changes in visual feedback gain on the dynamic of brain networks during precision grip, we recorded the mechanics and EEG signals during precision grip tasks under different levels of visual feedback gain (low, medium, high), and analyzed the EEG signals using microstate. The results showed that while precision grip performance significantly improved under medium/high gain, there were significant changes in EEG microstate. The findings of this study reveal that visual feedback gain may improve precision grip control by dynamically adjusting brain networks, indicating that moderate increases in visual feedback gain can significantly enhance the accuracy and stability of grip force. These findings are of significant importance in the field of rehabilitation medicine, especially in developing treatment strategies for patients with hand motor disorders. By adjusting visual feedback gain, it is possible to improve patients' hand motor performance, thus enhancing their daily living and work capabilities.

Acknowledgment

The authors declare that they have no competing interests.

References

[1] P. Arrighi et al., "EEG theta dynamics within frontal and parietal cortices for error processing during reaching movements in a prism adaptation study altering visuo-motor predictive planning," *PLoS ONE*, vol. 11, no. 3, Mar. 2016, Art. no. e0150265.

[2] C. M. Glazebrook, T. N. Welsh, and L. Tremblay, "The processing of visual and auditory information for reaching movements," *Psychol. Res.*, vol. 80, no. 5, pp. 757–773, Sep. 2016.

[3] R. J. Jagacinski and J. M. Flach, *Control Theory for Humans: Quantitative Approaches to Modeling Performance*. CRC Press, 2002, doi: 10.1201/9781315144948.

[4] J. W. Krakauer et al., "Differential cortical and subcortical activations in learning rotations and gains for reaching: A PET study," *J. Neurophysiol.*, vol. 91, no. 2, pp. 924–933, Feb. 2004.

[5] R. Caminiti, S. Ferraina, and P. B. Johnson, "The sources of visual information to the primate frontal lobe: A novel role for the superior parietal lobule," *Cerebral Cortex*, vol. 6, no. 3, pp. 319–328, 1996.

[6] S. P. Wise, D. Boussaoud, P. B. Johnson, and R. Caminiti, "Premotor and parietal cortex: Corticocortical connectivity and combinatorial computations," *Annu. Rev. Neurosci.*, vol. 20, no. 1, pp. 25–42, Mar. 1997.

[7] S. Li, A. Durand-Sanchez, and M. Latash, "Inter-limb force coupling is resistant to distorted visual feedback in chronic hemiparetic stroke," *J. Rehabil. Med.*, vol. 46, no. 3, pp. 206–211, 2014.

[8] P. Marcel-Millet, P. Gimenez, A. Groslambert, G. Ravier, and S. Grospretre, "The type of visual biofeedback influences maximal handgrip strength and activation strategies," *Eur. J. Appl. Physiol.*, vol. 121, no. 6, pp. 1607–1616, Mar. 2021.

[9] D. B. Archer, N. Kang, G. Misra, S. Marble, C. Patten, and S. A. Coombes, "Visual feedback alters force control and functional activity in the visuomotor network after stroke," *NeuroImage, Clin.*, vol. 17, pp. 505–517, Jan. 2018.

[10] D. E. Vaillancourt, K. R. Thulborn, and D. M. Corcos, "Neural basis for the processes that underlie visually guided and internally guided force control in humans," *J. Neurophysiol.*, vol. 90, no. 5, pp. 3330–3340, Nov. 2003.

[11] T. Watanabe, T. Mima, S. Shibata, and H. Kirimoto, "Midfrontal theta as moderator between beta oscillations and precision control," *NeuroImage*, vol. 235, Jul. 2021, Art. no. 118022.

[12] S. A. Coombes, D. M. Corcos, L. Sprute, and D. E. Vaillancourt, "Selective regions of the visuomotor system are related to gain-induced changes in force error," *J. Neurophysiology*, vol. 103, no. 4, pp. 2114–2123, Apr. 2010.

[13] P. Croce, F. Tecchio, G. Tamburro, P. Fiedler, S. Comani, and F. Zappasodi, "Brain electrical microstate features as biomarkers of a stable motor output," *J. Neural Eng.*, vol. 19, no. 5, Oct. 2022, Art. no. 056042.

[14] J. Schumacher et al., "Dysfunctional brain dynamics and their origin in Lewy body dementia," *Brain*, vol. 142, no. 6, pp. 1767–1782, Jun. 2019.

[15] D. Lehmann, H. Ozaki, and I. Pal, "EEG alpha map series: Brain microstates by space-oriented adaptive segmentation," *Electroencephalogr. Clin. Neurophysiol.*, vol. 67, no. 3, pp. 271–288, Sep. 1987.

[16] J. Britz, D. Van De Ville, and C. M. Michel, "BOLD correlates of EEG topography reveal rapid resting-state network dynamics," *NeuroImage*, vol. 52, no. 4, pp. 1162–1170, Oct. 2010.

[17] A. Custo, D. Van De Ville, W. M. Wells, M. I. Tomescu, D. Brunet, and C. M. Michel, "Electroencephalographic resting-state networks: Source localization of microstates," *Brain Connectivity*, vol. 7, no. 10, pp. 671–682, Dec. 2017.

[18] L. Bréchet, D. Brunet, G. Birot, R. Gruetter, C. M. Michel, and J. Jorge, "Capturing the spatiotemporal dynamics of self-generated, task-initiated thoughts with EEG and fMRI," *NeuroImage*, vol. 194, pp. 82–92, Jul. 2019.

[19] T. Chen et al., "Disrupted brain network dynamics and cognitive functions in methamphetamine use disorder: Insights from EEG microstates," *BMC Psychiatry*, vol. 20, no. 1, Dec. 2020, Art. no. 334.

[20] X. Chen et al., "The subsystem mechanism of default mode network underlying rumination: A reproducible neuroimaging study," *NeuroImage*, vol. 221, Nov. 2020, Art. no. 117185.

[21] E. Pirondini, M. Coscia, J. Minguillon, J. D. R. Millán, D. Van De Ville, and S. Micera, "EEG topographies provide subject-specific correlates of motor control," *Sci. Rep.*, vol. 7, no. 1, Oct. 2017, Art. no. 13229.

[22] Y. Fu, J. Chen, and X. Xiong, "Calculation and analysis of microstate related to variation in executed and imagined movement of force of hand clenching," *Comput. Intell. Neurosci.*, vol. 2018, Aug. 2018, Art. no. 9270685.

[23] R. C. Oldfield, "The assessment and analysis of handedness: The Edinburgh inventory," *Neuropsychologia*, vol. 9, no. 1, pp. 97–113, Mar. 1971.

[24] D. E. Vaillancourt, P. S. Haibach, and K. M. Newell, "Visual angle is the critical variable mediating gain-related effects in manual control," *Exp. Brain Res.*, vol. 173, no. 4, pp. 742–750, Aug. 2006.

[25] A. B. Slifkin and K. M. Newell, "Noise, information transmission, and force variability," *J. Exp. Psychol., Hum. Perception Perform.*, vol. 25, no. 3, pp. 837–851, 1999.

[26] D. H. Laidlaw, M. Bilodeau, and R. M. Enoka, "Steadiness is reduced and motor unit discharge is more variable in old adults," *Muscle Nerve*, vol. 23, no. 4, p. 600, Apr. 2000.

[27] H. Wang et al., "Differentiating propofol-induced altered states of consciousness using features of EEG microstates," *Biomed. Signal Process. Control*, vol. 64, Feb. 2021, Art. no. 102316.

[28] J. Liu, J. Xu, G. Zou, Y. He, Q. Zou, and J.-H. Gao, "Reliability and individual specificity of EEG microstate characteristics," *Brain Topography*, vol. 33, no. 4, pp. 438–449, Jul. 2020.

[29] A. T. Poulsen, A. Pedroni, N. Langer, and L. K. Hansen, "Microstate EEGLAB toolbox: An introductory guide," *bioRxiv*, Mar. 2018, doi: 10.1101/289850.

[30] R. D. Pascual-Marqui, C. M. Michel, and D. Lehmann, "Segmentation of brain electrical activity into microstates: Model estimation and validation," *IEEE Trans. Biomed. Eng.*, vol. 42, no. 7, pp. 658–665, Jul. 1995.

[31] J. Liu, X. Hu, X. Shen, Z. Lv, S. Song, and D. Zhang, "The EEG microstate representation of discrete emotions," *Int. J. Psychophysiol.*, vol. 186, pp. 33–41, Apr. 2023.

[32] T. Koenig, M. Kottlow, M. Stein, and L. Melie-García, "Ragu: A free tool for the analysis of EEG and MEG event-related scalp field data using global randomization statistics," *Comput. Intell. Neurosci.*, vol. 2011, no. 1, 2011, Art. no. 938925.

[33] T. Koenig et al., "Millisecond by millisecond, year by year: Normative EEG microstates and developmental stages," *NeuroImage*, vol. 16, no. 1, pp. 41–48, May 2002.

[34] Z. Zhao et al., "Causal link between prefrontal cortex and EEG microstates: Evidence from patients with prefrontal lesion," *Frontiers Neurosci.*, vol. 17, Dec. 2023, Art. no. 1306120.

[35] F. Zappasodi et al., "EEG microstates distinguish between cognitive components of fluid reasoning," *NeuroImage*, vol. 189, pp. 560–573, Apr. 2019.

[36] D. F. D'Croz-Baron, L. Bréchet, M. Baker, and T. Karp, "Auditory and visual tasks influence the temporal dynamics of EEG microstates during post-encoding rest," *Brain Topography*, vol. 34, no. 1, pp. 19–28, Jan. 2021.

[37] B. A. Seitzman, M. Abell, S. C. Bartley, M. A. Erickson, A. R. Bolbecker, and W. P. Hetrick, "Cognitive manipulation of brain electric microstate," *Neuroimage*, vol. 146, pp. 533–543, Feb. 2017.

[38] P. Milz, P. L. Faber, D. Lehmann, T. Koenig, K. Kochi, and R. D. Pascual-Marqui, "The functional significance of EEG microstates—Associations with modalities of thinking," *NeuroImage*, vol. 125, pp. 643–656, Jan. 2016.

[39] F. Callard, J. Smallwood, and D. S. Margulies, "Default positions: How neuroscience's historical legacy has hampered investigation of the resting mind," *Frontiers Psychol.*, vol. 3, Sep. 2012, Art. no. 321.

[40] D. A. Gusnard and M. E. Raichle, "Searching for a baseline: Functional imaging and the resting human brain," *Nature Rev. Neurosci.*, vol. 2, no. 10, pp. 685–694, Oct. 2001.

[41] P. Hagmann et al., "Mapping the structural core of human cerebral cortex," *PLoS Biol.*, vol. 6, no. 7, p. e159, Jul. 2008.

[42] V. Menon, "20 years of the default mode network: A review and synthesis," *Neuron*, vol. 111, no. 16, pp. 2469–2487, Aug. 2023.

[43] A. Jabès, G. Klencklen, P. Ruggeri, C. M. Michel, P. B. Lavenex, and P. Lavenex, "Resting-state EEG microstates parallel age-related differences in allocentric spatial working memory performance," *Brain Topography*, vol. 34, no. 4, pp. 442–460, Jul. 2021.

[44] M. M. Botvinick, T. S. Braver, D. M. Barch, C. S. Carter, and J. D. Cohen, "Conflict monitoring and cognitive control," *Psychol. Rev.*, vol. 108, no. 3, pp. 624–652, Jul. 2001.

[45] A. L. Ruiz-Rizzo, J. Neitzel, H. J. Müller, C. Sorg, and K. Finke, "Distinctive correspondence between separable visual attention functions and intrinsic brain networks," *Frontiers Hum. Neurosci.*, vol. 12, Mar. 2018, Art. no. 89.

[46] U. Korn et al., "EEG-microstates reflect auditory distraction after attentive audiovisual perception recruitment of cognitive control networks," *Frontiers Syst. Neurosci.*, vol. 15, Dec. 2021, Art. no. 751226.

[47] C. Fidalgo, N. M. Conejo, H. González-Pardo, and J. L. Arias, "Dynamic functional brain networks involved in simple visual discrimination learning," *Neurobiol. Learn. Memory*, vol. 114, pp. 165–170, Oct. 2014.

[48] M. Ekman, J. Derrfuss, M. Tittgemeyer, and C. J. Fiebach, "Predicting errors from reconfiguration patterns in human brain networks," *Proc. Nat. Acad. Sci. USA*, vol. 109, no. 41, pp. 16714–16719, 2012.